

# Limits to classification performance by relating Kullback-Leibler divergence to Cohen's Kappa

L. Crow, S. J. Watts\*

Department of Physics and Astronomy, The University of Manchester, Oxford Road, Manchester, M13 9PL, UK

## Abstract

The performance of machine learning classification algorithms are evaluated by estimating metrics, often from the confusion matrix, using training data and cross-validation. However, these do not prove that the best possible performance has been achieved. Fundamental limits to error rates can be estimated using information distance measures. To this end, the confusion matrix has been formulated to comply with the Chernoff-Stein Lemma. This links the error rates to the Kullback-Leibler divergences between the probability density functions describing two classes. This leads to a key result that relates Cohen's Kappa,  $\kappa$ , to the Resistor Average Distance,  $R(P, Q)$ , which is the parallel resistor combination of the two Kullback-Leibler divergences. The relation is,  $\kappa = 1 - 2^{-R(P, Q)}$ .  $R(P, Q)$  has units of bits and is estimated from the same training data used by the classification algorithm, using kNN estimates of the Kullback-Leibler divergences. The classification algorithm gives the confusion matrix and  $\kappa$ . Theory and methods are discussed in detail and then applied to Monte Carlo data and real datasets. Four very different real datasets (Breast Cancer, Coronary Heart Disease, Bankruptcy, and Particle Identification) are analysed, with both continuous and discrete values, and their performance compared to the expected theoretical limit given by the formula. In all cases this analysis shows that the algorithms could not have performed any better due to the underlying probability density functions for the two classes. Important lessons are learnt on how to predict the performance of algorithms for imbalanced data using training datasets that are approximately balanced. Machine learning is very powerful but classification performance ultimately depends on the quality of the data and the relevance of the variables to the problem.

Keywords: Kullback-Leibler, Chernoff-Stein Lemma, Cohen's Kappa, Classification, Imbalanced Classes

## Contents

<b>1</b>	<b>Introduction</b>	<b>2</b>
<b>2</b>	<b>Theory - Confusion matrix and error rates</b>	<b>2</b>
2.1	Confusion Matrix . . . . .	2
2.2	Cohen's Kappa . . . . .	3
2.3	Inter-relations between leakage rates and overall error rate . . . . .	4
<b>3</b>	<b>Theory - information divergence measures and error rates</b>	<b>4</b>
3.1	The Renyi Divergence, Resistor Average Distance, and the overall average error rate . . . . .	5
3.2	Link between the confusion matrix parameters and information theoretic distances . . . . .	6
3.3	Estimating the Kullback-Leibler Divergence from training data . . . . .	8
3.4	Summary of methodology and key equations . . . . .	8
<b>4</b>	<b>Application of the theory to data</b>	<b>8</b>
4.1	Monte Carlo simulation data . . . . .	9
4.2	Analysis of balanced Monte Carlo data . . . . .	9
4.3	Imbalanced Monte Carlo data . . . . .	9
4.4	Real datasets . . . . .	10
4.5	Key results and discussion . . . . .	11
4.5.1	Full application of the model to one variable in the breast cancer dataset . . . . .	11
4.5.2	Kappa for the full range of $f_1$ . . . . .	11
4.5.3	Overall average error, $K$ , and the Resistor Average Distance for real data . . . . .	11
4.5.4	Cohen's Kappa versus the Resistor Average Distance for real data . . . . .	12
<b>5</b>	<b>Conclusions</b>	<b>12</b>

---

\*Stephen.Watts@manchester.ac.uk

# 1 Introduction

The performance of machine learning algorithms applied to classification problems are evaluated by estimating parameters such as accuracy using training data and cross-validation. These methods provide good estimates of performance and are useful to compare the efficacy of different algorithms. Most performance parameters can be extracted from the confusion matrix which records how known classed instances are assigned by the algorithm to a classification. A perfect algorithm would result in a matrix with only diagonal entries. This subject is discussed in detail in ref. [1]. However, performance measures do not prove that the best possible performance has been achieved for a given dataset. They allow a comparison of different algorithms. This paper will provide a methodology to establish whether a classification algorithm has achieved the theoretical best case using information distance measures. It will concentrate on the binary or two-class classification problem. There is an extensive literature on how well one can classify observations from  $m$  possible classes dating back to the 1940's. The Neyman-Pearson and Bayes Decision Rules are much discussed, e.g. ref. [2], with the Bayes Decision Rule for minimum error leading to the concept of the Bayes Error Rate as the best one can achieve. These ideas can be discussed in either a Bayesian or Frequentist framework and lead to the same result. As Wasserman, ref. [3], notes "it is the nothing to do with Bayesian inference. The rule can be obtained using either Frequentist or Bayesian methods." The critical underlying idea is the likelihood ratio between the probability density functions (pdfs) for the two classes. Consideration of this ratio also led to the Kullback-Leibler Divergence, ref. [4], Chernoff-Stein Lemma, ref. [5], and Chernoff Information, ref. [6], all results within an information-theoretic framework, that are not dependent on prior probabilities. The relationship between key information distance measures are shown in Fig. 1 which is an expanded version of the one first drawn in ref. [7]. The figure includes the Renyi Divergence which will be shown in Section 3 to provide the key to solve the problem. If the pdf's are  $p(x)$  and  $q(x)$  for Class 1 and Class 2 instances, where a single variable  $x$  is used for clarity, but could also apply to a multivariate space, then the information measures labelled in Fig. 1 are related to the *exponential rates* for the optimal classification performance, [7]. The Neyman-Pearson error for fixed  $P_M$  is,

$$\lim_{N \rightarrow \infty} \frac{\log P_F}{N} = -D(P \parallel Q) \quad (1.1)$$

and the Chernoff Information,  $C(P, Q)$ , or bound on the Bayes Error is

$$\lim_{N \rightarrow \infty} \frac{\log P_E}{N} \leq -C(P, Q) \quad (1.2)$$

where,  $P_F$ ,  $P_M$  and  $P_E$  are the false alarm, miss and average error probabilities respectively. Equ. 1.1 is the Chernoff-Stein Lemma with  $D(P \parallel Q)$  being the Kullback-Leibler Divergence between the two pdf's. The Bhattacharyya Distance,  $B(P, Q)$  ref. [8], can also be used in Equ. 1.2. This bound is related to the Chernoff Information and  $B(P, Q) \leq C(P, Q)$ . For reference, in the Neyman-Pearson formulation,  $P_F$  would be a Type I Error or False Positive and  $P_M$  would be a Type II Error or False Negative. Since classification algorithms tend to treat classes equally and search for a minimum error solution, this paper will not use the Neyman-Pearson terminology. Equ. 1.1 and Equ. 1.2 show that the probability of error depends exponentially on these information divergence or distance measures. This will be used to formulate the confusion matrix such that it follows the Chernoff-Stein Lemma - Section 2.1. This matrix will be used to find a formula for Cohen's Kappa, a key performance measure which is often used to judge a classification algorithm - Section 2.2. One can then inter-relate and link the parameters of the confusion matrix with the information measures - Section 3.2. Finally, we estimate the information measures from the training data - Section 3.3. One can then compare the algorithm performance to the expected optimal prediction based on the information measures, which depend only on the underlying pdfs. This comparison delivers a verdict on whether the algorithm is performing as well as the underlying pdfs will permit. The theory summarised in Section 3.4 is then applied successfully to four real datasets and two simulated datasets in Section 4 and conclusions are given in Section 5. The methodology just described is shown diagrammatically in Fig. 2.

## 2 Theory - Confusion matrix and error rates

First we will describe the confusion matrix for a two class problem and ensure that it complies with the Chernoff-Stein Lemma. Then Cohen's Kappa will be introduced and expressed in terms of exponential rate parameters defining the confusion matrix. Note the units of the information measures are bits and nats if the logarithm base,  $b$ , is 2 or  $e$  respectively. The new formulation leads to important results that relate the key exponential rates.

### 2.1 Confusion Matrix

The confusion matrix will be written in a form that uses the Chernoff-Stein Lemma, with exponential rates for the false-alarm probability. In this section nats will be used. Consider a two class problem labelled by 1 and

2. In the training set there are  $N_1$  and  $N_2$  entries associated with these two classes. In a perfect world the classifier would generate a confusion matrix,  $\begin{bmatrix} N_1 & 0 \\ 0 & N_2 \end{bmatrix}$ . However, in the real world, a classification algorithm would not always correctly assign entries to the relevant class. The matrix can be written as,  $\begin{bmatrix} N_1^T & N_1^L \\ N_2^L & N_2^T \end{bmatrix}$  where,  $N_1^T$  and  $N_2^T$  are the entries correctly (“True”) assigned to Class 1 and 2 respectively, and  $N_1^L$  and  $N_2^L$  are the entries that “Leak” into the wrong Class. Thus,  $N_1^T + N_1^L = N_1$  and  $N_2^T + N_2^L = N_2$ . The total number of entries is,  $N = N_1 + N_2$ . This is shown diagrammatically in Fig. 3.

A random decision algorithm would assign class on the basis of the known number of entries in Class 1 and Class 2. The probability of a Class 1 entry is,  $\frac{N_1}{N_1+N_2}$ . The probability of a Class 2 entry is,  $\frac{N_2}{N_1+N_2}$ . Thus the “random” confusion matrix would be,  $\begin{bmatrix} N_1 \times \frac{N_1}{N} & N_1 \times \frac{N_2}{N} \\ N_2 \times \frac{N_1}{N} & N_2 \times \frac{N_2}{N} \end{bmatrix}$ . One now uses the Chernoff-Stein Lemma to describe the leaked entries subject to the constraint that the matrix take the form required by a random decision algorithm when the false-alarm rates are zero. The matrix has to be of the form,

$$\begin{bmatrix} N_1^T = N_1 - N_1^L & N_1^L = \frac{N_1 N_2}{N} \exp(-K_{12}) \\ N_2^L = \frac{N_1 N_2}{N} \exp(-K_{21}) & N_2^T = N_2 - N_2^L \end{bmatrix} \quad (2.1)$$

$K_{12}$  and  $K_{21}$  are the exponential rates that control the “leakage” of entries from Class 1 to Class 2 and from Class 2 to Class 1 respectively. They will be shown to be related to the Kullback-Leibler Divergence for the probability density functions describing the Class 1 and Class 2 entries.

## 2.2 Cohen’s Kappa

To date, over 26 performance measures, ref. [9], have been derived from the  $2 \times 2$  confusion matrix, although it only has two free parameters. We apply the matrix, Equ. 2.1, to calculate Cohen’s Kappa, ref. [10], which was originally intended to assess agreement between two judgements in psychological measurement. To quote ref. [10], it is the “proportion of agreement after chance agreement is removed”. When used in binary classification, it gives the efficiency of the algorithm after correcting for chance agreement. The confusion matrix defined in Equ. 2.1 is carefully formulated to take random agreement into account. The expression for Cohen’s Kappa,  $\kappa$ , is

$$\kappa = \frac{p_o - p_e}{1 - p_e} \quad (2.2)$$

where,  $p_o$  is the observed agreement and  $p_e$  is the agreement that one would find by random expectation. Note that  $1 - \kappa$  is the average probability that the classification is in error.  $\kappa$  can now be written in terms of the confusion matrix, Equ. 2.1. The observed agreement is,  $p_o = \frac{N_1^T + N_2^T}{N}$ . Random expectation for Class 1 is,  $p_1 = \frac{N_1}{N} \times \frac{N_1^T + N_2^L}{N}$ . Random expectation for Class 2 is,  $p_2 = \frac{N_2}{N} \times \frac{N_2^T + N_1^L}{N}$ . Then  $p_e = p_1 + p_2$ . Using these relations and after some algebra, one arrives at the relationship between  $\kappa$  and the parameters used in the matrix, Equ. 2.1.

$$\kappa = \frac{2N_1(1 - \exp(-K_{21})) + 2N_2(1 - \exp(-K_{12}))}{N_1(2 + \exp(-K_{12}) - \exp(-K_{21})) + N_2(2 + \exp(-K_{21}) - \exp(-K_{12}))} \quad (2.3)$$

There are two important limits for Equ. 2.3

1. When the classes are balanced,  $N_1 = N_2 = \frac{N}{2}$ ,  $\kappa = 1 - \frac{1}{2}(\exp(-K_{12}) + \exp(-K_{21}))$ . This only depends on two parameters and makes  $\kappa$  a robust statistic because there is no dependence on  $N_1$  or  $N_2$ .
2. When  $K_{12} = K_{21} \equiv K$ ,

$$\kappa = 1 - \exp(-K) \quad (2.4)$$

independent of  $N_1$  and  $N_2$ , e.g. imbalanced classes. Again  $\kappa$  is a robust statistic. This situation is not uncommon because a classification algorithm will do its best to optimize the efficiency for all classes, which will tend to make the rates similar.

The  $\kappa$  statistic has been criticised because of its dependence on how the  $N$  entries are balanced between  $N_1$  and  $N_2$ . Later it will be shown that this is inevitable and that this parameter correctly describes the classification performance, especially when the algorithm is looking to correctly classify both classes. Kappa is a key statistic describing the overall performance of the classification algorithm. Equ. 2.4 can be used to define the overall exponential error rate in terms of one parameter,  $K$  defined as,

$$K \equiv -\log_b(1 - \kappa) \quad (2.5)$$

### 2.3 Inter-relations between leakage rates and overall error rate

Once a classification algorithm has been applied to a training dataset, the resultant confusion matrix can be used to derive the three key parameters. The actual  $N_1^L$  and  $N_2^L$  elements can be used to estimate the  $K_{12}$  and  $K_{21}$  exponential leakage rates respectively using the formulae below and derived from Equ. 2.1.

$$K_{12} = -\log_b \left( \frac{1}{f_1 f_2 N} \cdot N_1^L \right) \quad (2.6)$$

$$K_{21} = -\log_b \left( \frac{1}{f_1 f_2 N} \cdot N_2^L \right) \quad (2.7)$$

where,  $f_1 \equiv \frac{N_1}{N}$  and  $f_2 \equiv \frac{N_2}{N}$  are the fraction of entries in Class 1 and Class 2 respectively. For this two class problem,  $f_1 + f_2 = 1$ . The overall rate,  $K$  is given by Equ. (2.5) and is estimated from a calculation of Cohen's Kappa. Since the confusion matrix has four elements and is constrained by knowledge of the number of Class 1 and Class 2 entries, there can only be two free parameters, and these three rates are related. To understand this, re-write Equ. 2.3 using Equ. 2.5 on the left-hand side,

$$1 - \exp(-K) = \frac{2N_1(1 - \exp(-K_{21})) + 2N_2(1 - \exp(-K_{12}))}{N_1(2 + \exp(-K_{12}) - \exp(-K_{21})) + N_2(2 + \exp(-K_{21}) - \exp(-K_{12}))} \quad (2.8)$$

Simplify this by assuming that  $|K_{12} - K|$  and  $|K_{21} - K| \lesssim 0.4$  nats or 0.6 bits. Then multiply the numerator and denominator of Equ. 2.8 by  $\exp(K)$ . After applying a Taylor expansion approximation to the  $\exp(K_{12} - K)$  and  $\exp(K_{21} - K)$  terms and some algebra one finds,

$$K \simeq f_1 K_{12} + f_2 K_{21} + \frac{1}{2}(1 - \exp(-K))(K_{21} - K_{12})(f_1 - f_2) \quad (2.9)$$

There are two solutions to Equ. 2.9

1. For balanced classes,  $f_1 = f_2 = \frac{1}{2}$ ,  $K \simeq f_1 K_{21} + f_2 K_{12} = \frac{1}{2}(K_{12} + K_{21})$ .
2. For symmetric Kullback-Leibler,  $K_{12} = K_{21}$ ,  $K \simeq f_1 K_{21} + f_2 K_{12}$ . In general, the last term is small compared to the first two factors, so one arrives at the same result.

In conclusion, there is an approximate relation between the three rates. This is exact for balanced classes or symmetric Kullback-Leibler divergence.

$$K_W \equiv f_1 K_{21} + f_2 K_{12} \simeq K \quad (2.10)$$

$K_W$  will be referred to as the *weighted error rate*. The confusion matrix is described in terms of these three parameters. These are the exponential average error rate ( $K$ ), exponential leakage rate causing Class 1 entries to be misclassified as Class 2 ( $K_{12}$ ), exponential leakage rate causing Class 2 entries to be misclassified as Class 1 ( $K_{21}$ ). As these descriptions are rather long, they will be referred to as the *average error rate*,  $K$ , and *leakage rates*  $K_{12}$  and  $K_{21}$ . Equ. 2.10 is a very important result. It is a rate equation because it relates these three rates and drives the classification algorithm which is designed to give the best value of  $K$  which itself is constrained by the Chernoff bound.

One final result from this formulation of the confusion matrix is that there is a limit to the leakage rate estimate. The smallest value of the off-diagonal entries in Equ. 2.6 or Equ. 2.7 is one. This puts a limit on the maximum leakage rate,

$$K_{Max}^L = \log_b N + \log_b(f_1 f_2) \quad (2.11)$$

This confirms a result in ref. [11], which found a  $\mathcal{O}(\log_b(N))$  limit on the Kullback-Leibler divergence. As this section shows, this is a consequence of the Chernoff-Stein Lemma.

## 3 Theory - information divergence measures and error rates

This section will derive in detail the relationships between the error rates and the information divergence measures and then relate these to the parameters,  $K$ ,  $K_{12}$ , and  $K_{21}$  of the confusion matrix. Next, it will show how to estimate the information distance measures independently from training data. The final sub-section returns to the overall methodology of the paper, which is shown schematically in Fig. 2, linking and referencing the key equations.

### 3.1 The Renyi Divergence, Resistor Average Distance, and the overall average error rate

Equ. 1.1 relates the leakage rate to the Kullback-Leibler divergence, which is a consequence of the Chernoff-Stein Lemma. The assumption of exponential error rates has been used in the formulation of the confusion matrix. However, one can only apply the Kullback-Leibler Divergence to a situation in which the classifier wishes to get the best performance for one class to the detriment of the other. This situation applies in signal detection when there is no interest in the noise. This corresponds to  $t = 0$  and  $t = 1$  in Fig. 1. Chernoff in ref. [6] realized that when treating each class equally, the answer lay between  $0 \leq t \leq 1$  with the Chernoff Information as a bound on the overall error rate. Ref. [7] proposed the Resistor Average Distance,  $R(P, Q)$ , as an estimate for this bound. This is the parallel resistor combination of  $D(P \parallel Q)$  and  $D(Q \parallel P)$ . It corresponds to the point where the two straight lines in Fig. 1 meet. These lines are the tangents to the Chernoff Divergence at  $t = 0$  and  $t = 1$  which have a slope of  $D(Q \parallel P)$  and  $D(P \parallel Q)$  respectively. In this section, the motivation for  $R(P, Q)$  will be explained in terms of the Renyi Divergence rather than using the argument in Ref. [7]. The Renyi Divergence is a generalization of the Kullback-Leibler Divergence and is described in detail in ref. [12], which also describes the hypothesis testing problem in terms of the Renyi Divergence. It is defined as follows,

$$D_t(P \parallel Q) \equiv \frac{1}{t-1} \log \int_S p(x) \left( \frac{p(x)}{q(x)} \right)^{t-1} dx = \frac{1}{t-1} \log \int_S p(x)^t q(x)^{1-t} dx \quad (3.1)$$

The middle form clearly shows the link to the likelihood ratio,  $\frac{p(x)}{q(x)}$ . The final form is the one most often used. The log term is due to Chernoff from which the overall error bound was derived. Nowadays, it is often referred to as the Chernoff Divergence, ref. [13], which is,

$$C_t(P \parallel Q) = (t-1)D_t(P \parallel Q) \quad (3.2)$$

The Chernoff Information or Distance is,

$$C(P, Q) \equiv \text{Max}(C_t(P \parallel Q)) \quad (3.3)$$

This occurs at a value of  $t = t_c$ , which is indicated in Fig. 1. Only values of the Renyi and Chernoff Divergence for  $0 \leq t \leq 1$  are of interest in this paper, in which case,  $C_t(P \parallel Q) = C_{1-t}(Q \parallel P)$ . See ref. [12] for other values of  $t$ . From the definitions it is easy to show that,

$$(1-t)D_t(P \parallel Q) = tD_{1-t}(Q \parallel P) = C_t(P \parallel Q) \quad (3.4)$$

This is called Skew Symmetry, ref. [12], and is a key property of the Renyi Divergence from which the concept of Resistor Average Distance appears naturally. Finally, the Kullback-Leibler Divergence is,

$$D(P \parallel Q) \equiv \int_S p(x) \log \left( \frac{p(x)}{q(x)} \right) dx \quad (3.5)$$

which is  $D_t(P \parallel Q)$  at  $t = 1$ . Note also that  $D(Q \parallel P) = D_{1-t}(Q \parallel P)$  at  $t = 0$ . The relationships between Kullback-Leibler Divergence and Chernoff Divergence are shown in Fig. 1. The Resistor Average Distance is defined mathematically as,

$$(1-t)D(P \parallel Q) = tD(Q \parallel P) = R(P, Q) \quad (3.6)$$

Equ. 3.6 is of the same form as the Skew Symmetry property given in Equ. 3.4. These have similar solutions. The Resistor Average Distance is the point,  $t = t_R$ , at which the two tangential lines meet in Fig. 1,

$$R(P, Q) = \frac{D(P \parallel Q)D(Q \parallel P)}{D(P \parallel Q) + D(Q \parallel P)} \quad (3.7)$$

or

$$\frac{1}{R(P, Q)} = \frac{1}{D(P \parallel Q)} + \frac{1}{D(Q \parallel P)} \quad (3.8)$$

The solution for the Chernoff Divergence for  $0 \leq t \leq 1$ ,

$$C_t(P \parallel Q) = \frac{D_t(P \parallel Q)D_{1-t}(Q \parallel P)}{D_t(P \parallel Q) + D_{1-t}(Q \parallel P)} \quad (3.9)$$

or

$$\frac{1}{C_t(P, Q)} = \frac{1}{D_t(P \parallel Q)} + \frac{1}{D_{1-t}(Q \parallel P)} \quad (3.10)$$

To link  $R(P, Q)$  with the Chernoff Divergence, take a first-order approximation to the Renyi Divergence that  $D_t(P \parallel Q) \simeq tD(P \parallel Q)$  and  $D_{1-t}(Q \parallel P) \simeq (1-t)D(Q \parallel P)$ . This is an equality for a symmetric Kullback-Leibler Divergence, i.e  $D(P \parallel Q) = D(Q \parallel P)$ . This approximates the Renyi Divergences with two lines which

are related to the tangential lines in Fig. 1 when exchanging  $t \longleftrightarrow 1 - t$  and  $P \leftrightarrow Q$ . Substituting in Equ. 3.9 gives,

$$C_t(P \parallel Q) = \frac{tD(P \parallel Q)(1-t)D(Q \parallel P)}{tD(P \parallel Q) + (1-t)D(Q \parallel P)} \quad (3.11)$$

Evaluate Equ. 3.11 at  $t = 0.5$  which is the Bhattacharyya Distance, which is known to be close the Chernoff Distance, then,

$$C_{1/2}(P \parallel Q) = B(P, Q) = \frac{R(P, Q)}{2} \quad (3.12)$$

For a symmetric Kullback-Liebler Divergence,  $D(P \parallel Q) = D(Q \parallel P)$

$$R(P, Q) = 2C_{1/2}(P, Q) = 2C(P, Q) = 2B(P, Q) = D_{1/2}(P \parallel Q) = \frac{D(P \parallel Q)}{2} \quad (3.13)$$

A second order fit to the Renyi Divergence can be written as,

$$D_t(P \parallel Q) = tD(P \parallel Q) + At(1-t), D_{1-t}(Q \parallel P) = (1-t)D(Q \parallel P) + Bt(1-t) \quad (3.14)$$

This is the only form compatible with the boundary conditions at  $t = 0$  and  $t = 1$ . Since these divergences meet at  $t = 0.5$  one finds that,

$$A = 4D_{1/2}(P \parallel Q) - 2D(P \parallel Q), B = 4D_{1/2}(Q \parallel P) - 2D(Q \parallel P) \quad (3.15)$$

The curves drawn in Fig. 1 are for the exponential model described in Section 4.1 for which  $A = 0.2269$  and  $B = -0.4342$ . Simple algebra starting with Equ. 3.15 finds that,

$$D_{1/2}(P \parallel Q) = D_{1/2}(Q \parallel P) = R(P, Q) \left[ 1 + \frac{A}{4D(P \parallel Q)} + \frac{B}{4D(Q \parallel P)} \right] \quad (3.16)$$

Since  $A$  and  $B$  are small compared to  $D(P \parallel Q)$  and  $D(Q \parallel P)$  respectively, and have opposite sign,  $R(P, Q)$  is a good estimate of the Renyi Divergence at  $t = 0.5$ . The correction term in square brackets in Equ. 3.16 for the exponential model is 0.991. The second order approximation to the Renyi divergence, Equ. 3.14 is used to estimate the Chernoff divergence, Equ. 3.11, and this is shown in Fig. 1. There is good agreement with the calculated Chernoff divergence. Equ. 3.16 also suggests that  $D_{1/2}(P \parallel Q)$  is the information distance measure relevant to the overall error rate since it is half way between the solutions at  $t = 0$  ( $D(Q \parallel P)$ ) and  $t = 1$  ( $D(P \parallel Q)$ ) which correspond to attaining the best error for just one of the classes. In mathematical terms, the *conjecture* is that,

$$\lim_{N \rightarrow \infty} \frac{\log P_E}{N} \simeq -D_{1/2}(P \parallel Q) \simeq -R(P, Q) \quad (3.17)$$

One can also write Equ. 1.1 as,

$$\lim_{N \rightarrow \infty} \frac{\log P_F}{N} = -D_1(P \parallel Q) = D(P \parallel Q) \quad (3.18)$$

The value of  $t$  at which  $R(P, Q)$  occurs, Fig. 1, is

$$t_R = \frac{D(P \parallel Q)}{D(P \parallel Q) + D(Q \parallel P)} \quad (3.19)$$

This conjecture is borne out by application to data in Section 4 and a mathematical result in the next section which shows from the confusion matrix parameterisation, underpinned by the Chernoff-Stein Lemma, that  $K$  at  $t = t_R$  is  $R(P, Q)$ . Referring back to ref. [6] and using modern terminology, it notes that the Chernoff Divergence and Kullback-Leibler Divergence are two different functionals on a curve relating Type 1 and Type 2 errors for likelihood ratio tests. The Renyi Divergence is another functional which provides the link between the Type 1 and Type 2 errors and also the Bayes Error when the classifier works well on both classes.

### 3.2 Link between the confusion matrix parameters and information theoretic distances

Associate  $P$  and  $Q$  with Class 1 and Class 2 respectively. The two rates that define the confusion matrix are  $K_{12}$  and  $K_{21}$ , so the classifier will minimise the overall average error rate by keeping  $K \simeq R(P, Q)$  but must ensure that  $K \simeq f_1 K_{21} + f_2 K_{12}$  which was shown earlier, Equ. 2.10. We will consider two cases.

1. The Kullback-Leibler Divergence is symmetric. The Renyi Divergence will be linear and Equ. 3.13 will apply. Thus  $K = D_{1/2}(P \parallel Q) = R(P, Q) = \frac{D(P \parallel Q)}{2} = \frac{D(Q \parallel P)}{2}$ . This occurs at  $t = 0.5$  and if the classes are balanced then,  $K_{12} = K_{21} = K$  due to Equ. 2.10. This is an exact solution. If the classes are imbalanced,  $f_1 \neq f_2$  then  $K_{12} \neq K_{21}$  but the classification algorithm will try to preserve the value of  $K$ . This can be understood by considering the extremes. When extrapolating  $f_1 \rightarrow 1$  there are only Class 1 entries. In this case, one applies the Chernoff-Stein lemma, Equ. 1.1, and  $K_{12} \simeq D(Q \parallel P)$ , which corresponds to  $t = 1$ . When extrapolating,  $f_1 \rightarrow 0$  there are only Class 2 entries, and in this case, one applies the Chernoff-Stein lemma, Equ. 1.1, and  $K_{21} \simeq D(P \parallel Q)$ , which corresponds to  $t = 0$ . In this case,  $D(P \parallel Q) = D(Q \parallel P)$ , but the argument applies to the asymmetric case too. One is thus led to write the following formulae for  $K_{12}$  and  $K_{21}$ ,

$$K_{12} \sim D(2, 1)f_1, K_{21} \sim D(1, 2)f_2 \quad (3.20)$$

This provides a solution to the classification problem for the three key values of  $t = 0$ ,  $t = 0.5$ , and  $t = 1$ , which correspond respectively to the Chernoff-Stein, Chernoff Bound, and Chernoff-Stein solutions and  $t$  directly maps to the fraction of entries in Class 1,  $f_1$ . The parameters  $D(1, 2)$  and  $D(2, 1)$  are estimated from data and should correspond to the underlying values  $D(P \parallel Q)$  and  $D(Q \parallel P)$  respectively. Fig. 1 is the key to this conclusion. Combining Equ. 2.10 and Equ. 3.20 one finds that,

$$K \simeq K_W = f_1 f_2 D(1, 2) + f_2 f_1 D(2, 1) = f_1(1 - f_1)(D(1, 2) + D(2, 1)) \quad (3.21)$$

This immediately shows why one can preserve a constant  $K$  and that the maximum value of  $K$  will be at  $f_1 = \frac{1}{2}$ . There will be a region of  $f_1$  when  $K$  will be *roughly* constant and the classification will apply to both classes. At the extremes, when the classes are severely imbalanced, this may no longer apply. This will be discussed later. Results from simulations, shown later, indicate that one needs to modify Equ. 3.20, with an extra correction term, that is linked to the overlap between the two classes.

$$K_{12} = \Delta_1 + (D(2, 1) - \Delta_1)f_1 \quad (3.22)$$

$$K_{21} = \Delta_2 + (D(1, 2) - \Delta_2)f_2 = D(1, 2) - (D(1, 2) - \Delta_2)f_1 \quad (3.23)$$

where,  $0 \leq \Delta_1 \leq D(2, 1)$  and  $0 \leq \Delta_2 \leq D(1, 2)$ . For the symmetric case,  $D(1, 2) = D(2, 1)$ ,  $\Delta_1 = \Delta_2$  and  $K_{12} = K_{21}$ . The value of  $f_1$  when  $K_{12} = K_{21}$  will be called the *balance point*, which in this case is,  $f_B = 0.5$ . Despite the more complicated equations for  $K_{12}$  and  $K_{21}$ , it is simple to show that the maximum value of  $K$  is still at  $f_1 = 0.5$  provided  $\Delta_1$  and  $\Delta_2$  are much smaller than  $D(1, 2)$  and  $D(2, 1)$ .

2. The Kullback-Leibler Divergence is not symmetric. The overall error rate will still be controlled by  $K = R(P, Q)$ . Equ. 3.22 and Equ. 3.23 will still apply. This balance point can be approximated well as,

$$f_B \simeq \frac{D(1, 2)}{D(1, 2) + D(2, 1)} \left[ 1 + \frac{\Delta_1 + \Delta_2}{D(1, 2) + D(2, 1)} - \frac{\Delta_1}{D(1, 2)} \right] \quad (3.24)$$

This works well because  $\Delta_1$  and  $\Delta_2$  are small compared to  $D(1, 2)$  and  $D(2, 1)$ . Moreover, one can see immediately that,

$$f_B \approx t_R \quad (3.25)$$

The balance point for the two error rates is the same as the value of  $t$  at which the Resistor Average Distance is determined. This further justifies the link between the  $f_1$  and  $t$ . One can estimate the value of  $K$  at the balance point. To clearly illustrate the result, the problem will be simplified with  $\Delta_1 = \Delta_2 = 0$ . At the balance point,  $f_1 = \frac{D(1, 2)}{D(1, 2) + D(2, 1)}$  and  $f_2 = \frac{D(2, 1)}{D(1, 2) + D(2, 1)}$ . Putting these into Equ. 3.21, one finds,

$$K \simeq K_W = \frac{D(1, 2)}{D(1, 2) + D(2, 1)} \bullet \frac{D(2, 1)}{D(1, 2) + D(2, 1)} \bullet (D(1, 2) + D(2, 1)) = \frac{D(1, 2)D(2, 1)}{D(1, 2) + D(2, 1)} = R(P, Q) \quad (3.26)$$

This returns us to the start of this section, and justifies the underlying model that the algorithm will try its best to maintain  $K = R(P, Q)$  while keeping  $K \simeq f_1 K_{21} + f_2 K_{12}$ . This is an approximation but works well in the region of  $f_1$  when it is possible to classify both classes adequately. This region will depend upon the underlying pdfs. The application section will show how one can determine the region in  $f_1$  that permits a reasonable two-class classification. Using units of bits, an equation that can be checked for all data, re-writes Equ. 2.4 as,

$$\kappa \simeq 1 - 2^{-R(P, Q)} = 1 - 2^{-CDR} \quad (3.27)$$

This important equation connects the classification performance with that expected from the independently estimated information distance measure for  $R(P, Q)$ .  $CDR$  is the  $k^{th}$  nearest-neighbour (kNN) estimate of  $R(P, Q)$  which is described in Section 3.3. It should work well at the balance point and more generally in the region where the algorithm can classify both classes.

### 3.3 Estimating the Kullback-Leibler Divergence from training data

The Kullback-Leibler Divergence is estimated from the same training data used by the classification algorithm but with an independent method that only considers the underlying pdfs. The use of kNN non-parametric estimators of entropy was initiated by the work of ref. [14]. The application to divergence was made by ref. [15]. These methods produce an estimate that is consistent and unbiased. Assigning Class 1 and Class 2 entries to distributions  $P$  and  $Q$  respectively and using ref. [15] we write the estimate of  $D(P \parallel Q)$  in bits as,

$$CDI(1,2) = \frac{d}{N_1} \sum_{i=1}^{i=N_1} \log_2 \left( \frac{\lambda_i^{12}}{\lambda_i^1} \right) + \log_2 \left( \frac{N_2}{N_1 - 1} \right) \quad (3.28)$$

This is called the Class Distance Indicator between Class 1 and Class 2 entries to make it clear that it is an *estimate* of the Kullback-Leibler Divergence between these two distributions. It uses the kNN distances which are defined as follows,

- $\lambda_i^1$  is the nearest neighbour distance between the  $i^{th}$  point in Class 1 and all the other Class 1 points.
- $\lambda_i^{12}$  is the nearest neighbour distance between the  $i^{th}$  point in Class 1 and all Class 2 points.
- $d$  is the number of variables or dimensionality of the data space.

Equ. 3.28 deals automatically with imbalanced classes due to the second term. This equation is applied to binned data with the bin value converted to a real value by adding a uniform random number between zero and one. This allows one to use the same algorithm for discrete, continuous and mixed data. Moreover, the  $CDI$  can be estimated multiple times and then averaged. This reduces the error and provides a lower bound on the error for one computation. For continuous data the binning uses an algorithm that ensures each variable has the same Shannon entropy. This reduces systematic errors. A detailed paper is in preparation but one can obtain further information on the method and its performance in refs. [16, 17, 18]. The Resistor Average Distance,  $R(P, Q)$ , is estimated by a parameter called,  $CDR$ , which is the parallel resistor combination of  $CDI(1, 2)$  and  $CDI(2, 1)$ ,

$$\frac{1}{CDR} = \frac{1}{CDI(1,2)} + \frac{1}{CDI(2,1)} \quad (3.29)$$

### 3.4 Summary of methodology and key equations

The methodology of this paper is summarised in Fig. 2. The aim was to link the performance of a classification algorithm on training data with the underlying pdfs. This has been achieved by estimating key information distance measures from the same training data, independently of the classification algorithm. These distances allow the prediction of the best achievable performance which can be compared to the actual performance. Referring to Fig. 2,

- The classification algorithm performance is summarised in terms of its confusion matrix and Cohen's Kappa. Section 2 showed how the key parameters,  $K$ ,  $K_{12}$  and  $K_{21}$  are extracted using Equ. 2.5, Equ. 2.6 and Equ. 2.7 respectively.
- The relationship between the information measures and the error rates in Equ. 1.1 and Equ. 1.2 are described in Section 3. The estimates of the information measures for  $D(P \parallel Q)$ ,  $D(Q \parallel P)$  and  $R(P, Q)$  are  $CDI(1,2)$ ,  $CDI(2,1)$  and  $CDR$  respectively. These are described in Section 3.3. One can also estimate the information measures by fitting the  $K_{12}$  and  $K_{21}$  results, extracted from an analysis of the confusion matrix resulting from the classification algorithm, namely,  $D(1, 2)$  and  $D(2, 1)$ , Eqs. 3.22 and 3.23 respectively.
- The model for the confusion matrix parameters is described in Section 3.2. The key results are Equ. 3.22, Equ. 3.23, Equ.3.26 and Equ. 3.27.

Fig. 2 contains key equations and links to the text. The next section uses these results to evaluate how well this theory and model work on simulated and real datasets.

## 4 Application of the theory to data

Table 1 is a summary of the six datasets, refs. [17, 19, 20, 21], to which the theory and model described in Section 2 and Section 3 are applied. The key equations are summarised in Fig. 2 and Section 3.4. The datasets are of three types. S1 and S2 are Monte Carlo generated data based on Gaussian and Exponential distributions. D1, D3 and D4 are datasets available on public websites. D2 has been used before and is described in Ref. [17]. S1, S2, D1 and D3 use continuous variables. D2 has only discrete variables. D4 is a mixed dataset with one discrete variable. These datasets are described in Section 4.1 and 4.4 and then analysed in Sections 4.2, 4.3, and 4.5. Version 3.9.6 of the WEKA, [1], machine learning software was used. The classification algorithm used in WEKA is given in Table 1. The algorithm was chosen on the basis of its performance with each dataset using standard defaults in WEKA.

## 4.1 Monte Carlo simulation data

S1 and S2 are balanced datasets with  $f_1 = f_2 = 0.5$ . They were generated because one can solve these problems numerically from the equations defining the pdfs. Each dataset has 16 variables, each of which uses the same pdf, and these variables are generated independently. There is no shared mutual information between the variables. The S2 exponential model was used to calculate the information measures that are shown in Fig. 1. The mathematical form is given in Equ. 4.2, from which the divergences were calculated numerically. A Bayes Network classification algorithm was chosen to process the data. For both datasets the Bayes Network algorithm showed the WEKA software had correctly identified that all variables were only dependent on the class variable. This algorithm should perform optimally for these datasets. If  $p_i(x)$  and  $q_i(x)$  are the pdf's for the  $i^{th}$  variable for class 1 and class 2 respectively, with  $i = 1$  to 16, then for the Gaussian dataset S1, the distributions are,

$$p_i(x) = N(0, 1), q_i(x) = N(1.02, 1) \quad (4.1)$$

where  $N(\mu, \sigma)$  is a Gaussian distribution with mean,  $\mu$ , and standard deviation,  $\sigma$ . With this choice one can show that for a single variable,  $D(P \parallel Q) = D(Q \parallel P) = 0.75$  bits and  $R(P, Q) = 0.375$  bits. For the exponential distribution the choice of pdf's are,

$$p_i(x) = \frac{1}{\alpha} \exp(-\frac{x}{\alpha}), q_i(x) = \frac{1}{\beta} \exp(-\frac{x}{\beta}) \quad (4.2)$$

with  $\alpha = 1$  and  $\beta = 2.392$ . With this choice one can show that for a single variable,  $D(P \parallel Q) = 0.42$  bits,  $D(Q \parallel P) = 0.75$  bits and  $R(P, Q) = 0.27$  bits. Due to independence, as the variables are combined, the total  $D(P \parallel Q)$ ,  $D(Q \parallel P)$  and  $R(P, Q)$  will be the values stated multiplied by the number of variables used. This allowed 16 different values of increasing dimensionality to be processed by both the information distance measure software as well as the corresponding classification results when using WEKA. Table 2 tabulates which figures show the results from processing the simulated data; V1 means one variable, V1V2 means the two variables, V1 and V2, etc. Generating such data uses well known techniques. Ref. [18] provides more detail.

## 4.2 Analysis of balanced Monte Carlo data

The Monte Carlo models have  $N_1 = N_2 = \frac{N}{2}$ , which is referred to as *balanced* classes. Fig. 4a) shows the relationship between  $K$ ,  $K_{12}$ , and  $K_{21}$  for the Gaussian simulated data described in Section 4.1. The average of  $K_{12}$  and  $K_{21}$  is also plotted. Since the Gaussian model has a symmetric Kullback-Leibler Divergence and  $f_1 = f_2 = 0.5$  one finds that  $K = K_{12} = K_{21} = \frac{1}{2}(K_{12} + K_{21})$ , as expected. Fig. 4b) repeats the exercise for the exponential simulated data described in Section 4.1. The Kullback-Leibler Divergence is not symmetric and  $K_{12} \neq K_{21}$  because  $D(Q \parallel P) \neq D(P \parallel Q)$ . As expected, the average,  $\frac{1}{2}(K_{12} + K_{21})$  equals  $K$ .

Fig. 5 shows the estimated Kullback-Leibler Divergences,  $CDI(1, 2)$ ,  $CDI(2, 1)$ , and Resistive Average Distance,  $CDR$ , for the a) Gaussian model and b) Exponential model. The lines show the expected theoretical values which are linear in the number of variables because these they are independent.  $CDI$  and  $CDR$  use a double and single line respectively. For the Gaussian model  $CDI(1, 2) = CDI(2, 1)$  since the Kullback-Leibler Divergence is symmetric. Fig. 5 a) shows that the  $CDI$  and  $CDR$  are lower than expected for more than 5 variables. This is due to the unfortunately named “*curse of dimensionality*”, ref. [22]. There are two related aspects to this problem. First, the number of samples required to estimate an arbitrary function to a given accuracy grows exponentially with dimensionality. Points are most likely to be found close to the surface and the full phase space is not used. Second, ref. [23], the distance of a point to its nearest neighbour tends to a constant as the dimensionality increases. The Kullback-Leibler Divergence depends on the ratio of two nearest neighbour distances, Equ. 3.28, so is affected as the number of variables increases. This problem has been studied by the authors and a correction found. Due to the extra pages required this is not described here especially as it is a small perturbation to the main aim of this paper. Moreover, it is found that the classification algorithms also suffer from the curse and the uncorrected  $CDR$  remains a reliable estimate of the underlying error rate which is demonstrated by analysis of the datasets described in this paper. Fig. 5b) shows the calculation for the exponential model. As the underlying Kullback-Leibler divergences are different, the behaviour of  $CDI(1, 2)$  and  $CDI(2, 1)$  are quite different due to the dimensionality. Below 8 variables,  $CDI(2, 1) > CDI(1, 2)$  as expected. However, beyond 8 variables, the relationship switches. This does not occur to the confusion matrix parameters,  $K_{12}$  and  $K_{21}$  which remain correctly ordered for all dimensions. The  $CDR$  remains a good estimate of the overall error rate.

## 4.3 Imbalanced Monte Carlo data

Real data rarely has balanced classes, a situation called *imbalanced classes*, i.e.  $f_1 \neq f_2$ . Moreover, the imbalance in the training data may be very different to real life. For example,  $f_1 = 0.37$  for the Breast Cancer data, but in reality the probability for such a cancer in the general population is considerably lower. The uncorrected rate for women in the UK between 2016-18 was 166 per 100,000 of the population, ref. [24]. The probability for women

to be diagnosed with this cancer, during their lifetime, is about 1 in 7. When either  $f_1$  or  $f_2$  are 0.01 or smaller, the data set is said to be in *Severe Imbalance*. This is a well known problem, and care must be taken to train the classification algorithm for such a situation, see ref. [25]. Cohen's Kappa is sensitive to imbalance. Equ. 2.3 clearly shows the  $N_1$  and  $N_2$  dependence which is irrelevant when  $K_{12} = K_{21}$  or the classes are balanced,  $N_1 = N_2$ . In Fig. 4 the classes were balanced for both the Gaussian and Exponential models. The exercise of obtaining the confusion matrix parameters and information measures was repeated for different values of  $f_1$  for both the Gaussian and Exponential models with four variables only. From Section 4.1, one would expect that  $CDI(1,2) = CDI(2,1) = 4 \times 0.75 = 3.0$  bits for the Gaussian model. For the Exponential Model one would expect  $CDI(1,2) = 0.42 \times 4 = 1.68$  bits and  $CDI(2,1) = 0.75 \times 4 = 3.0$  bits. Fig. 6a) shows the confusion matrix parameters,  $K$ ,  $K_{12}$  and  $K_{21}$  and the information distance measures,  $CDI(1,2)$  and  $CDI(2,1)$ , versus the fraction of Class 1 entries,  $f_1$ . This figure is symmetric about  $f_1 = 0.5$  because  $D(P \parallel Q) = D(Q \parallel P)$ . The information distance measures are independent of  $f_1$  showing that the correction factor in Equ. 3.28 works well. There is remarkable resemblance between Fig. 6 and Fig. 1 with  $f_1$  clearly related to the parameter  $t$ . This is not a surprise because  $f_1 = 0$  corresponds to the error rate being maximal for Class 2 entries, which is the Chernoff-Stein Lemma, Equ. 1.1, with  $K_{21} = D(P \parallel Q) = CDI(1,2)$ . The situation is reversed for  $f_1 = 1$  or  $f_2 = 0$  with  $K_{12} = D(Q \parallel P) = CDI(2,1)$ .  $K_{12}$  and  $K_{21}$  vary linearly between the two extremes and are equal at  $f_1 = f_2 = 0.5$ . For severely imbalanced classes, one can apply the Chernoff-Stein Lemma, Equ. 1.1 but not Equ. 1.2. An overall error rate only makes sense when one is trying to identify both classes as well as possible and they must be reasonably balanced. In this case, this corresponds to  $0.2 < f_1 < 0.8$ . Fig. 6b) shows parameters that describe the overall performance derived from the confusion matrix -  $\kappa$  and  $K$  - and the information distance measure,  $CDR$ . In the region of reasonable balance, there is agreement between  $K$  and the CDR. Using Equ. 3.27, the expected value of  $\kappa$  can be plotted. There is good agreement between this and the actual  $\kappa$  in the region of reasonable balance. The weighted error rate,  $K_W$ , Equ. 2.10, is also shown in Figs. 6 b) and 7 b). This agrees remarkably well with the actual  $K$ . The parametrisations for  $K_{12}$  and  $K_{21}$  were then fitted to both Figs. 6a) and 7a). The results are shown in Table 3. Table 4 gives the information distance measures for the same datasets. There is good agreement between the various estimates and the expected theoretical values. This shows that the underlying theory and model is working well. There is good agreement between the balance points ( $K_{12} = K_{21}$ ) and that expected from Equ. 3.19 and Equ. 3.24, confirming again the link between  $f_1$  and Chernoff's  $t$ .

#### 4.4 Real datasets

As the simulated data has independent variables the choice of which to combine and use is simple. In real datasets the variables share information and thus the choice of which combinations to show is problematic. There are  $2^p - 1$  combinations for  $p$  variables. Only for the D2 dataset have all been processed. In other cases, most of the single variables, two variable combinations and selected combinations were processed. These are detailed in Table 2. The selected variables were chosen as follows. First, find the single variable with the largest  $CDR$ . Combine this with the next variable which increases  $CDR$  the most. Continue this process until the  $CDR$  is unchanged by adding unused variables. One then has a list of  $N_s$  selected variables ordered by increasing  $CDR$ . The number of combinations to check are  $\frac{1}{2}(p-1)(p+2)$ , which is considerably less than before. Moreover, the classification algorithm is only applied  $N_s$  times. This paper is not a detailed analysis of the datasets. They are being used to confirm the methodology. Table 1 contains references to each data source. Brief information for each dataset is given below.

1. The breast cancer data, D1, has 30 continuous variables, ref. [19]. There is a high degree of correlation between the variables and the number needed to successfully classify the data was found to be 7. This data has been widely studied and other choices of variables have been found. Due to the shared information between the variables this is not surprising. The selection algorithm discussed above gave the following ordered list of variables; perimeter worst, concave points mean, radius worst, radius mean, perimeter mean, area mean, texture worst. The class variable is Malign (M) or Benign (Be).
2. The bankruptcy data, D2, has 6 discrete variables, ref. [20]. All 63 combinations were processed for classification results and information distance measures. The class variable is Bankrupt (Bk) or Not Bankrupt (NBk).
3. The Particle Physics data, D3, has 8 continuous variables, ref. [17]. It is the result of a sophisticated Monte Carlo simulation to understand real physics data. The selection algorithm gave the following ordered list of variables; Fsig, Sfl, Rxy, Rz, Doca, Cos-Hel, Pchi, Mass. The final variable was added last because in the real experiment one would use the classification to identify the particle, and then confirm its mass. This variable would not be used in the initial classification algorithm. The class variable is Signal (S) or Background (B).
4. The Coronary Heart Disease data, D4, is the result of a health study in South Africa. This has 8 continuous and 1 discrete variable, ref. [21]. As will be shown, one cannot achieve a high classification performance with this data. All single variable, all double variable, and a mix of 3 variable and 4 variable combinations

were processed. Higher variable combinations actually give worse performance and were not included. The class variable is No Disease (ND) or Coronary Heart Disease (CHD).

## 4.5 Key results and discussion

### 4.5.1 Full application of the model to one variable in the breast cancer dataset

Fig. 8 shows the behaviour of  $K_{12}$  and  $K_{21}$  versus  $f_1$  for the Breast Cancer dataset for just one variable. This was chosen because it is real data and illustrates that the methodology works well even though there are only 579 total entries. The most important variable, “perimeter worst” is analyzed as one can display its pdf using a histogram, shown in Fig. 8a). The Kullback-Leibler divergences were estimated using Equ. 3.28 and found to be  $CDI(1,2)= 5.2$  bits and  $CDI(2,1)= 3.43$  bits. The distributions for the two classes have a different mean, which will give a non-zero Kullback-Leibler divergence, but it is asymmetric because they have different variances. This dataset has  $f_1 = 0.37$ . Other values of  $f_1$  were obtained as follows;  $f_1 < 0.37$ ,  $N_2$  was kept at its initial value of 357 and entries from Class 1 were reduced; for  $f_1 > 0.37$ ,  $N_1$  was kept at its initial value of 212 and entries from Class 2 were reduced. Analysis of these different values of  $f_1$  is shown in Fig. 8b). This figure shows  $K_{12}$ ,  $K_{21}$ ,  $K$  and  $CDR$  as a function of  $f_1$ . The values of  $CDI(1,2)$  and  $CDI(2,1)$  are placed at  $f_1 = 0$  and  $f_1 = 1$  respectively as this corresponds to a situation in which one is only interested in performance for one class. The balance point,  $f_R \simeq t_R = 0.57$ , is indicated by a vertical broken line. For Fig. 8b) from the fit  $\Delta_1 = (1.32 \pm 0.24)$  bits,  $CDI(2,1) = (3.13 \pm 0.2)$  bits,  $\Delta_2 = (0.84 \pm 0.27)$  bits, and  $CDI(1,2) = (4.66 \pm 0.2)$  bits. The independent kNN estimate of  $CDI(1,2) = 5.2$  bits and  $CDI(2,1) = 3.43$  bits. These were included in the fit to the points in Fig. 8 b) although the results are compatible within the errors when they are excluded. These results are included in Table 3 and Table 4. The weighted error rate is also shown in Fig. 8b) and again shows good agreement with the actual  $K$ . There is excellent consistency between all these results which confirm the underlying methodology. The same method can be used for multiple dimensions. This example was chosen because one can easily show the pdf for one variable.

### 4.5.2 Kappa for the full range of $f_1$

Table 3 provides all the parameters needed to calculate Cohen’s kappa across the full range of  $f_1$  for two Monte Carlo datasets and the perimeter worst variable for the Breast Cancer data. One can extrapolate to find its value at both extremes which would normally not be possible with small datasets. These parameters plus Equ. 3.22 and 3.23 are required. The calculated  $K_{12}$  and  $K_{21}$  are used to estimate  $\kappa$  using Equ. 4.3, which is a reformulation of Equ. 2.3 to make the dependence on  $f_1$  and  $f_2$  clearer. From Equ. 2.3 one can derive the following formula which uses units of bits.

$$\kappa = \frac{2(1 - f_1 2^{-K_{21}} - f_2 2^{-K_{12}})}{2 + Z(f_1 - f_2)}, Z = 2^{-K_{12}} - 2^{-K_{21}} \quad (4.3)$$

This formula better illustrates the limits when  $f_1 = f_2$  or  $K_{12} = K_{21}$ , already discussed in Section 2.2. Using this formula and the numbers in Table 3, one obtains Fig. 9. Important conclusions can be drawn from this figure about the meaning of  $\Delta_1$  and  $\Delta_2$ , used in Equ. 3.22 and Equ. 3.23. The Gaussian Model has class distributions that are offset with the same variance. There is an overlap of the classes but not for the whole range of either class.  $\kappa$  is symmetric about  $f_1 = 0.5$  and  $\Delta_1 = \Delta_2 \neq 0$  because they do not fully overlap.  $\kappa$  is non-zero at the extremes, and there is some evidence that the classification algorithm is not working correctly at the extremes of  $f_1$ . The perimeter worst class distributions are offset and have different variances. There is an overlap of classes but not for the whole range.  $\kappa$  is not symmetric about  $f_1 = 0.5$ . Moreover,  $\Delta_1 \neq \Delta_2$  and are non-zero because they do not fully overlap and consequently,  $\kappa$  is non-zero at the extremes. The Exponential Model has class distributions that overlap. Class 1 is completely overlapped by Class 2. However, Class 2 has some part of its range in which the overlap is very unlikely. This is the reason why  $\Delta_1 = 0$  and  $\Delta_2 > 0$ . Consequently as  $f_1 \rightarrow 0$ ,  $K_{12} \rightarrow 0$  and  $\kappa \rightarrow 0$ . When the number of Class 1 entries is very low then if they occur they will be classified as Class 2. A different outcome happens at  $f_1=1$  because  $\Delta_2 > 0$  then  $K_{21} > 0$  and  $\kappa$  is non-zero. When the number of Class 2 entries is very low then if they occur the algorithm can still classify some entries correctly because they are more likely to be outside the range of Class 1 entries. This shows the importance that pdf’s should not fully overlap if the algorithm is to work at low numbers of entries. This example illustrates that  $\Delta_1$  and  $\Delta_2$  are a measure of whether a class is fully separated from other classes;  $\Delta = 0$  means they fully overlap.

### 4.5.3 Overall average error, $K$ , and the Resistor Average Distance for real data

Fig. 10 is a key result of this paper. The overall error rate, described by  $K$ , which is derived from Cohen’s Kappa,  $\kappa$ , which is obtained from the confusion matrix describing the result of the machine learning classification algorithm, is plotted versus the  $CDR$  which is an estimate of the Resistor Average Distance  $R(P, Q)$ , and also  $D_{1/2}(P \parallel Q)$ . Both simulated data and the real datasets are on this plot. Despite the very different nature of the datasets, there is a good linear correlation between these parameters. This figure plus the background theory gives confidence that Equ. 3.17 applies in general which is also confirmed by the derivation of Equ. 3.26.

#### 4.5.4 Cohen’s Kappa versus the Resistor Average Distance for real data

Fig. 11 is the most important result. The goal of the work was to relate the performance of the classification algorithm with expectation from the underlying pdf’s, using the same training data. This figure shows this goal has been achieved. Cohen’s Kappa, which is a performance measure of the classification algorithm, agrees with the *CDR* information distance measure. The curve in the figure is Equ. 3.27. The real datasets have been plotted in this figure and show excellent agreement with Equ. 3.27. A wide range of different numbers of variables with differing kappa were chosen to show that each dataset agreed across a wide range of *CDR*. The same classification algorithm was used for any mix of variables. A kappa scale taken from ref. [26] shows that all datasets achieve very good classification, except for the coronary heart disease data. The inability to classify the heart disease data more effectively is due to a lack of discrimination in the variables required to achieve a high *CDR* and thus a significant kappa. This figure shows there is no need to search for a new algorithm that might give an improved result. However, there are links between the variables and coronary heart disease that give non-zero *CDR*. This data is useful for risk analysis, which historically was how it was analyzed, which in turn led to a public health programme that improved outcomes for this disease in South Africa, ref. [27].

## 5 Conclusions

- To our knowledge, this is the first time that the performance of machine learning classification algorithms has been compared with an information distance measure, estimated independently from the underlying probability density functions of the two classes using the same training data. The information distance measure provides a best case performance estimate so one can check that the machine learning algorithm is optimal.
- The methodology applies to discrete, continuous or mixed data. Performance for imbalanced classes has been understood and related to the underlying information distances. The methodology works for any number of variables although more work is required to understand both the information distance measures and classification algorithm at high dimensions.
- The methodology allows one to understand how well an algorithm should perform when the class imbalance is severe, which is the case for many real world problems.
- No algorithm, no matter how clever, can better the performance limit set by the information distance measures. For example, the coronary heart disease (CHD) data is only able to deliver “Fair” performance. This type of data is useful for risk analysis but not prediction.
- The methodology can be applied to multi-class data by taking the classes in pairs. In principle, the confusion matrix parametrization could be extended to a multi-class problem.

## Acknowledgements

LC thanks UKRI (STFC) and The University of Manchester for research student funding. SW thanks the Leverhulme Trust for their support with an Emeritus Fellowship.

## References

- [1] E. Frank, M. Hall, I. Witten (2016), “ The WEKA Workbench” , Morgan Kaufmann, Fourth Edition
- [2] A. Webb and K. Copsey (2011), “Statistical Pattern Recognition”, John Wiley and Sons, Third Edition.
- [3] L. Wasserman (2004), “ All of statistics ”, Springer texts in statistics.
- [4] S. Kullback (1997), “ Information theory and statistics”, Dover Publications Inc.
- [5] H. Chernoff, “ Large-sample theory: Parametric Case” (1956) Ann. Math. Stat. 27(1), 1-22.
- [6] H. Chernoff, “A measure of asymptotic efficiency for tests of a hypothesis based on a sum of observations” (1952) Ann. Math. Stat. 23(4), 493-507.
- [7] S. Sinanovic and D. Johnson, “Toward a theory of information processing”, Signal Processing (2007) 87(6), 1326-1344.
- [8] A. Bhattacharyya, “On a Measure of Divergence between Two Multinomial Populations “, (1946) Indian Journal Stats. 7(4), 401-406.

- [9] L. Nieto and A. Correndo, “Classification performance metrics and indices” (2023), R project documentation, [https://cran.r-project.org/web/packages/metrica/vignettes/available\\_metrics\\_classification.html](https://cran.r-project.org/web/packages/metrica/vignettes/available_metrics_classification.html), Accessed 4 December 2023.
- [10] J. Cohen, “ A coefficient of agreement for nominal scales” (1960) Educational and Psychological Measurement, XX(1), 37-46.
- [11] D. McAllester and K. Stratos, “ Formal limitations on the measurement of mutual information”, (2020), Proceedings 23rd AISTATS Conference, Palermo, Vol 108.
- [12] T. van Erven and P. Harresmoes, “Renyi Divergence and Kullback-Leibler Divergence” (2014) 60(7) 3797-3820.
- [13] G. E. Crooks, “ On measures of entropy and information”, (2021) Tech. Note 009 v0.8, <http://threepluseone.com/info>, Accessed 4 December 2023.
- [14] L. Kozachenko and N. Leonenko , “ Sample Estimate of the Entropy of a Random Vector ” (1987) Problems Inform. Transmission 23:2, 95-101.
- [15] Q. Wang et al., “ Divergence Estimation for Multidimensional Densities Via  $k$ -Nearest-Neighbor Distances ” (2009) IEEE Trans. Information Theory, 55, 2392-2405.
- [16] Lisa Crow, “A novel approach to estimating information-theoretic measures for exploratory data analysis and explainable machine learning” (2022) PhD Thesis, University of Manchester, <https://www.escholar.manchester.ac.uk/uk-ac-man-scw:332338>.
- [17] S J. Watts & L. Crow, “ Big Variates: Visualizing and identifying key variables in a multivariate world” (2019) Nuclear Instruments and Methods in Physics Research A: 940, 441-447.
- [18] S. J. Watts and L. Crow, “ The Shannon Entropy of a Histogram “ (2022) <https://doi.org/10.48550/arXiv.2210.02848>
- [19] W. N. Street, W. H. Wolberg and O. L. Mangasarian. “ Nuclear feature extraction for breast tumor diagnosis “ (1993) IS&T/SPIE International Symposium on Electronic Imaging: Science and Technology, volume 1905, pages 861-870, San Jose, CA.
- [20] Kim and Han, “ The Discovery of Experts’ Decision Rules from Quantitative Data Using Genetic Algorithms “ (2003) Expert Systems with Applications, 25, 637-646.
- [21] J. E. Rossouw et al., “ Coronary risk factor screening in three rural communities - the CORIS baseline study “ (1983) South African Medical Journal, 64, 430-436.
- [22] R. Bellman, “Adaptive Control Processes” (1961) Princeton University Press.
- [23] K. Beyer, J. Goldstein, R. Ramakrishnan, and U. Shaft. “ When is ‘nearest neighbor’ meaningful ? ” (1999) Proc. Int. Conf. Database Theory, 217-235
- [24] Data from <https://www.cancerresearchuk.org/>, accessed on 22 January 2024.
- [25] A. Fernandez, S. Garcia, M. Galar, R. Prati, B. Krawczyk, F. Herrera, “Learning from Imbalanced Data Sets” (2018), Springer.
- [26] D. G. Altman “ Practical statistics for medical research ” (1991) Chapman and Hall, London, pp. 404
- [27] T. Hastie, R. Tibshirani and J. Friedman, “The Elements of Statistical Learning: Data Mining, Inference, and Prediction” (2009) Second Edition (Springer Series in Statistics)

# FIGURES

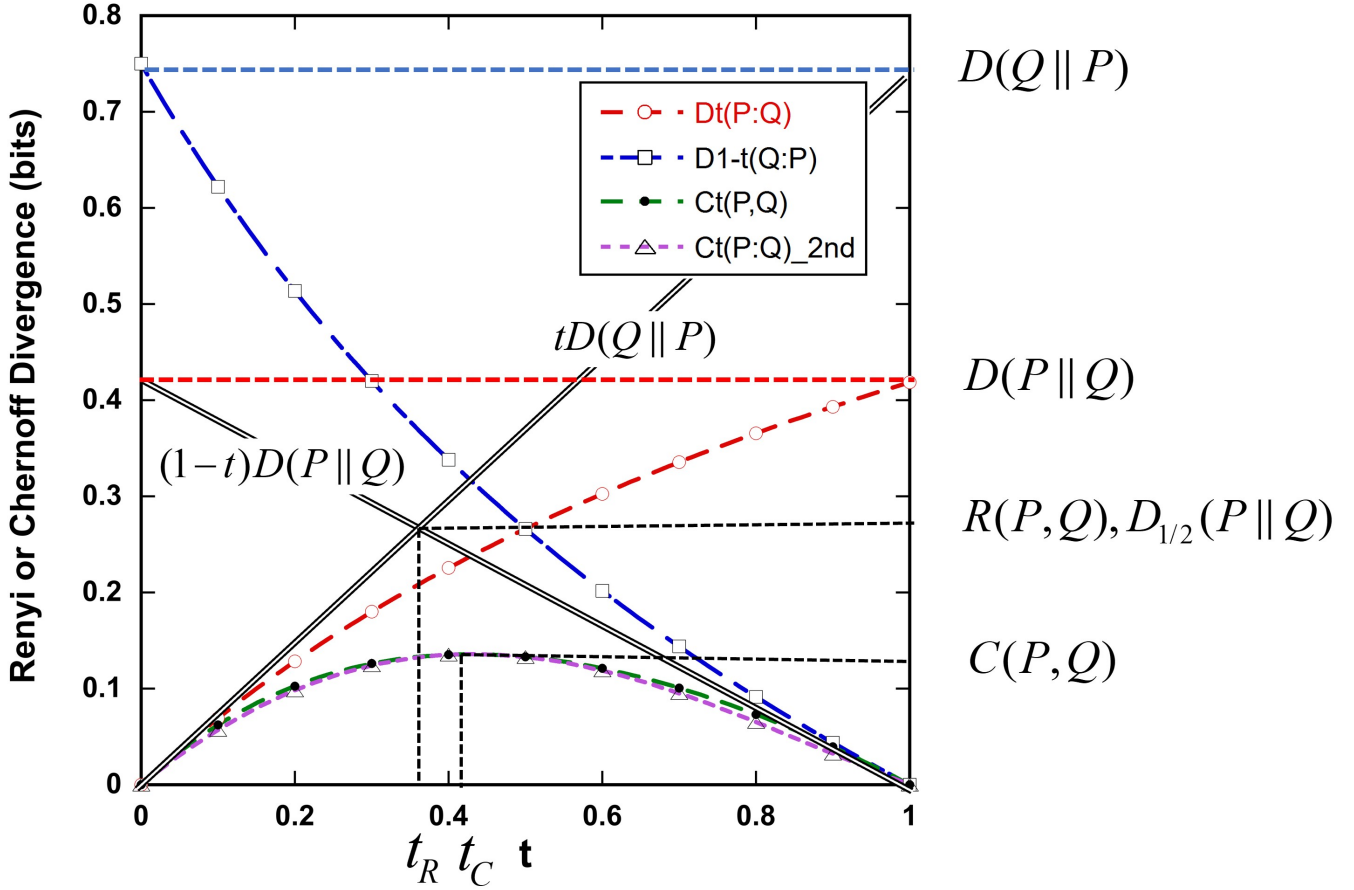


Figure 1: This figure is an update of one used in ref. [7] to show the relationships between key information theoretic distances. The curves are for a 1D exponential model described in Section 4.1. Renyi Divergences,  $D_t(P || Q)$  and  $D_{1-t}(Q || P)$ , Chernoff Divergence,  $C_t(P || Q)$ , Kullback-Leibler Divergences,  $D(P || Q)$  and  $D(Q || P)$ . The Resistor Average Distance,  $R(P, Q)$ , [7], is at  $t = t_R$  and Chernoff Information,  $C(P, Q)$ , is at  $t = t_C$ .  $R(P, Q)$  is the value at which the two double lines meet. These are tangential to the Chernoff Divergence at  $t = 0$  and  $t = 1$ . The Renyi Divergence at  $t = 1/2$ ,  $D_{1/2}(P || Q) = D_{1/2}(Q || P)$ , has a value close to  $R(P, Q)$ . This is not an accident as the main text explains. Not shown on figure, but for reference, the Bhattacharyya Distance,  $B(P, Q)$  is the value of the Chernoff Divergence at  $t = 1/2$ , which is  $\frac{1}{2}D_{1/2}(P || Q)$ . A second order approximation to the Renyi divergence is used to estimate the Chernoff Divergence, which is shown in the figure. See Section 3.1 for details.

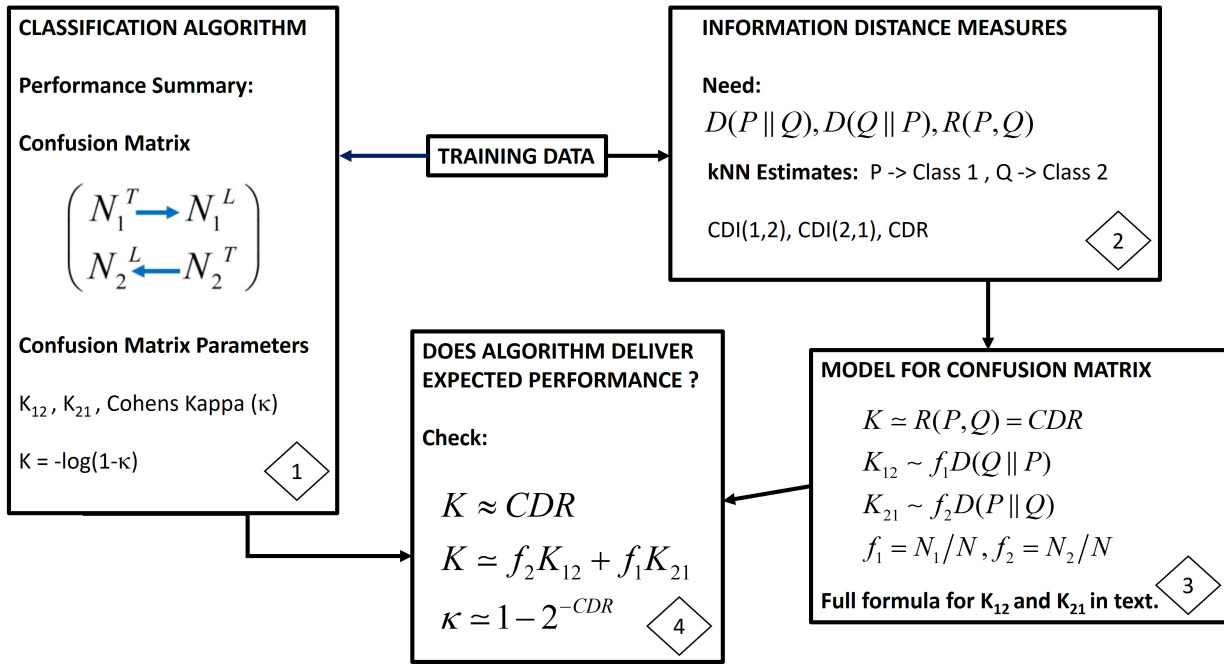


Figure 2: Methodology to compare performance of a classification algorithm with expectation from information distance measures. For full details in the main text; Box 1 see Section 2, Box 2 see Sections 3.1 and 3.3, Box 3 see Section 3.2, Box 4 see Sections 3.2 and 3.3.

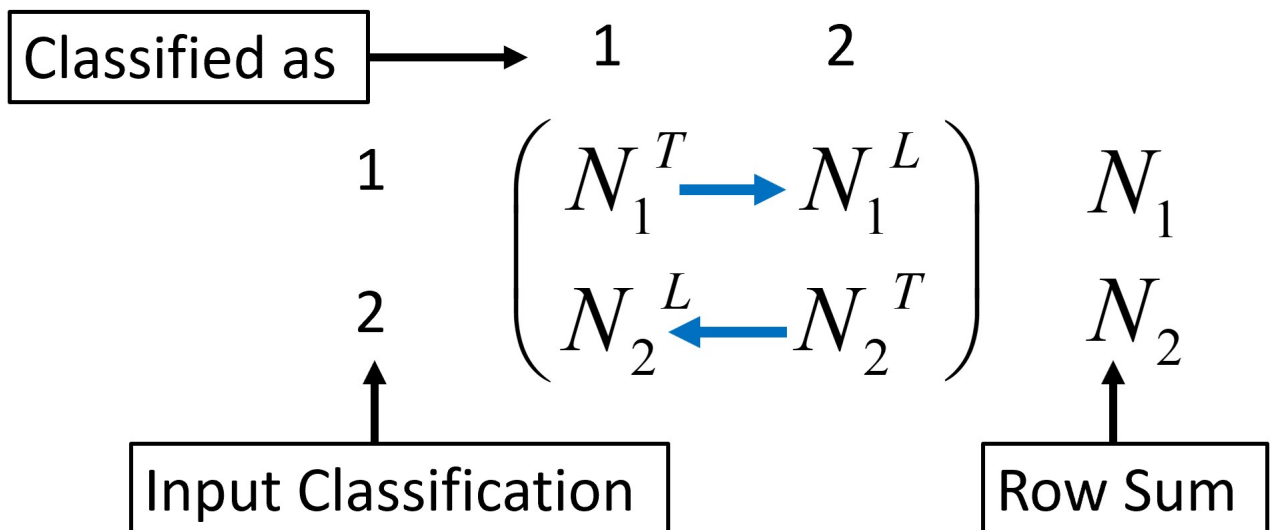


Figure 3: Definition of the two class confusion matrix. The arrows indicate how entries “leak” from their true class (T) to the wrong class (L).

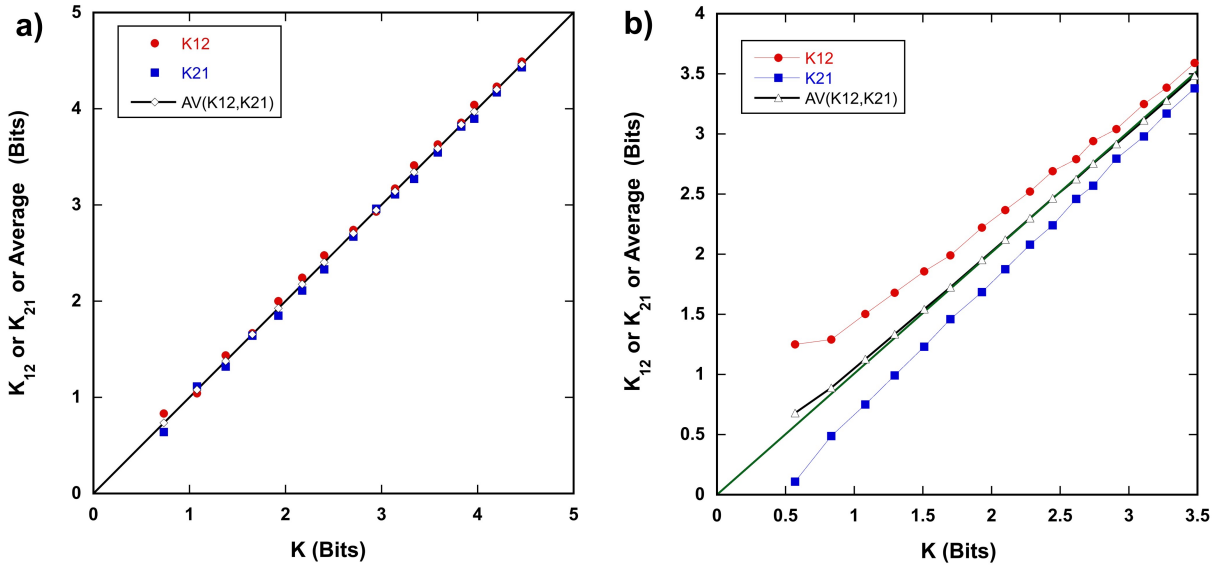


Figure 4: a) Relationships between the parameters  $K$ ,  $K_{12}$  and  $K_{21}$  and average ( $1/2(K_{12} + K_{21})$ ) for the Gaussian Model. Slope of line is 1.0 for all. b) Repeat for the Exponential Model. Slope of line for average is 1.0. This is for balanced data,  $f_1 = f_2 = 0.5$ . The models are described in Section 4.1.

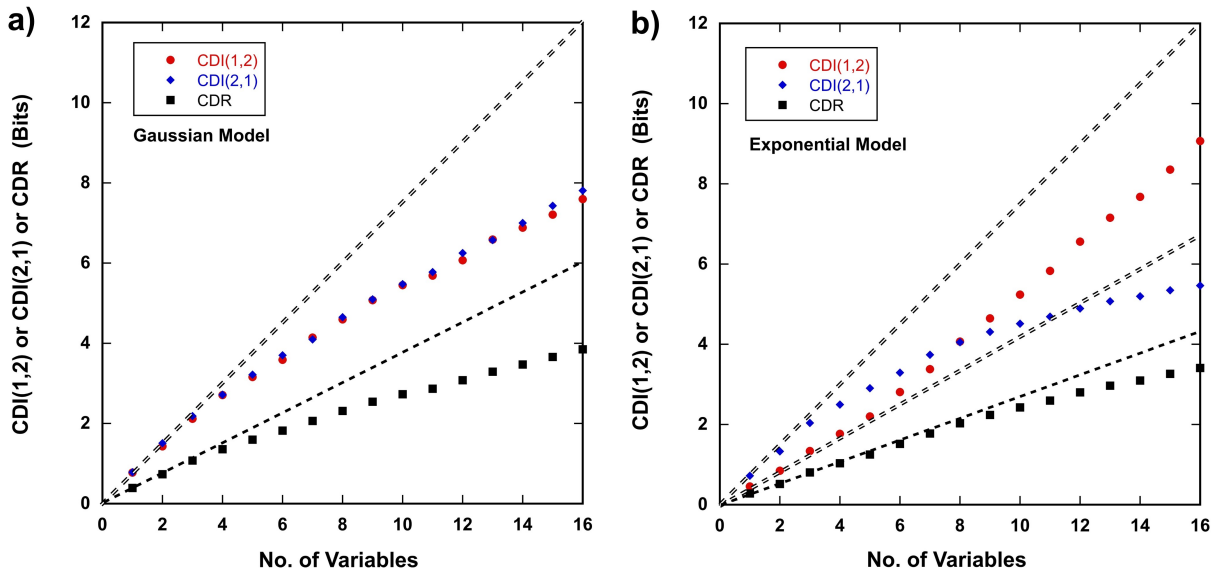


Figure 5: kNN estimates of the Kullback-Leibler Divergences,  $CDI(1,2)$  and  $CDI(2,1)$ , and Resistor Average Distance,  $CDR$ , for both the Gaussian and Exponential models. See Sections 3.3 and 4.2 for detail. Double dashed lines are the theoretical prediction for the Kullback-Leibler divergence. Single dashed lines are the theoretical prediction for the Resistor Average Distance.

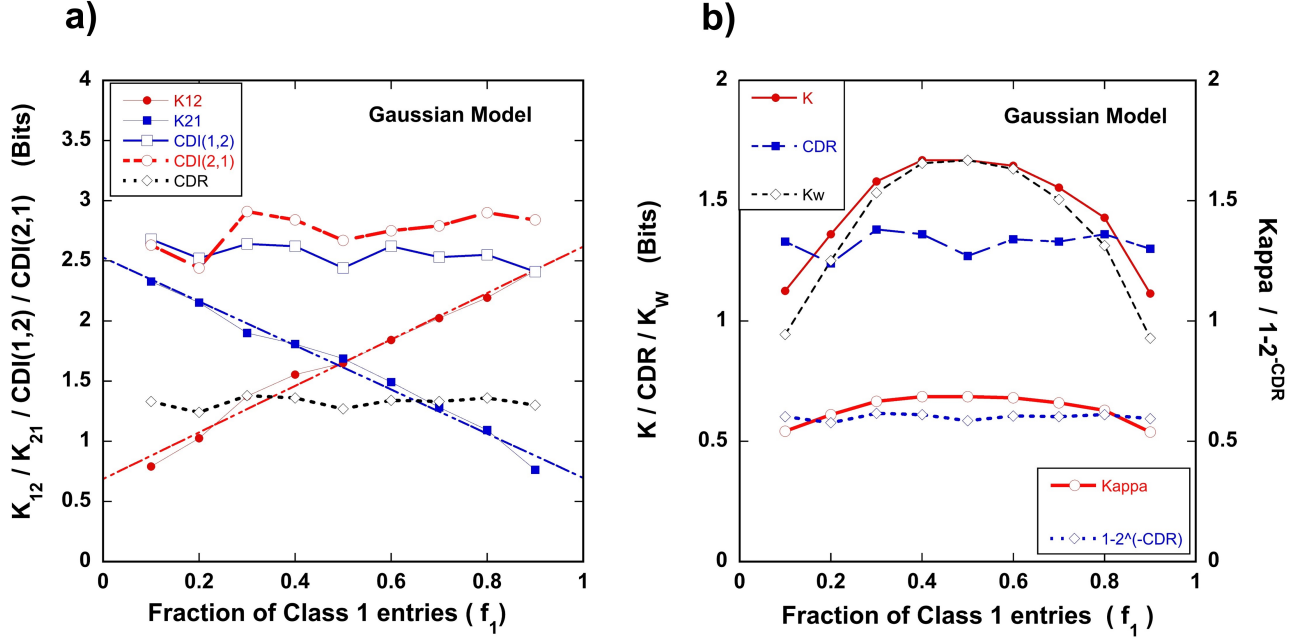


Figure 6: a)  $K_{12}, K_{21}, CDI(1,2), CDI(2,1)$  versus the fraction of Class 1 entries for the Gaussian Model. This illustrates how the leakage rates tend to the Kullback-Leibler Divergence for  $D(Q \parallel P)$  and  $D(Q \parallel P)$  for  $f_1 = 1$  and  $f_1 = 0$  respectively. This is consistent with Equ. 1.1 which is a statement of the Chernoff-Stein Lemma. b) Left-hand axis,  $K, CDR$ , and the weighted error rate,  $K_W$ . Right-hand axis, Cohen's Kappa,  $\kappa$ , and  $1 - 2^{-CDR}$ . Both versus the fraction of Class 1 entries for the Gaussian Model. The variables on the right-hand axis have a maximum value of one but the range is set to avoid a clash between the left-hand and right-hand points. There is reasonable agreement between  $K$  and  $CDR$ . There is better agreement between Cohen's Kappa and  $1 - 2^{-CDR}$ . There is good agreement between  $K$  and  $K_W$  supporting Equ. 2.10 .

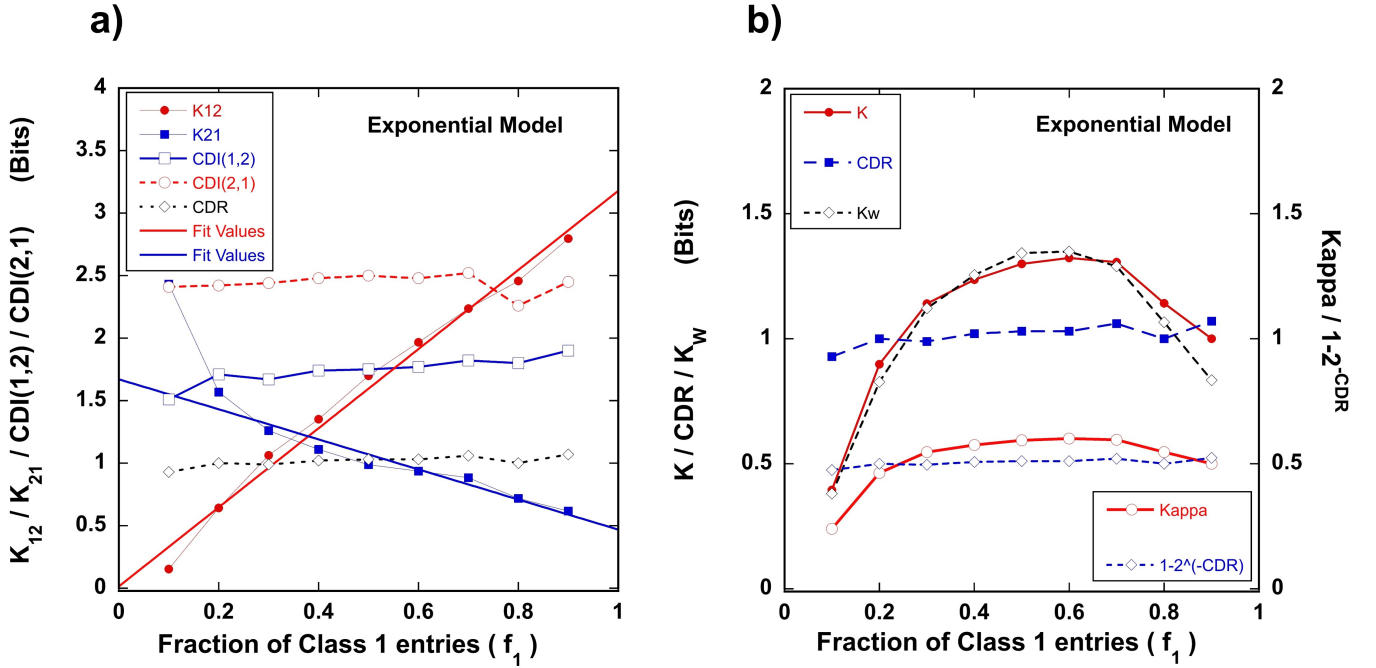


Figure 7: Repeat of Fig. 6 for the Exponential Model. a)  $K_{12}, K_{21}, CDI(1,2), CDI(2,1)$  versus the fraction of Class 1 entries. b) Left-hand axis,  $K, CDR$ , and the weighted error rate,  $K_W$ . Right-hand axis, Cohen's Kappa,  $\kappa$ , and  $1 - 2^{-CDR}$ . Both versus the fraction of Class 1 entries. The variables on the right-hand axis have a maximum value of one but the range is set to avoid a clash between the left-hand and right-hand points. There is reasonable agreement between  $K$  and  $CDR$ . There is better agreement between Cohen's Kappa and  $1 - 2^{-CDR}$ . There is good agreement between  $K$  and  $K_W$  supporting Equ. 2.10 .

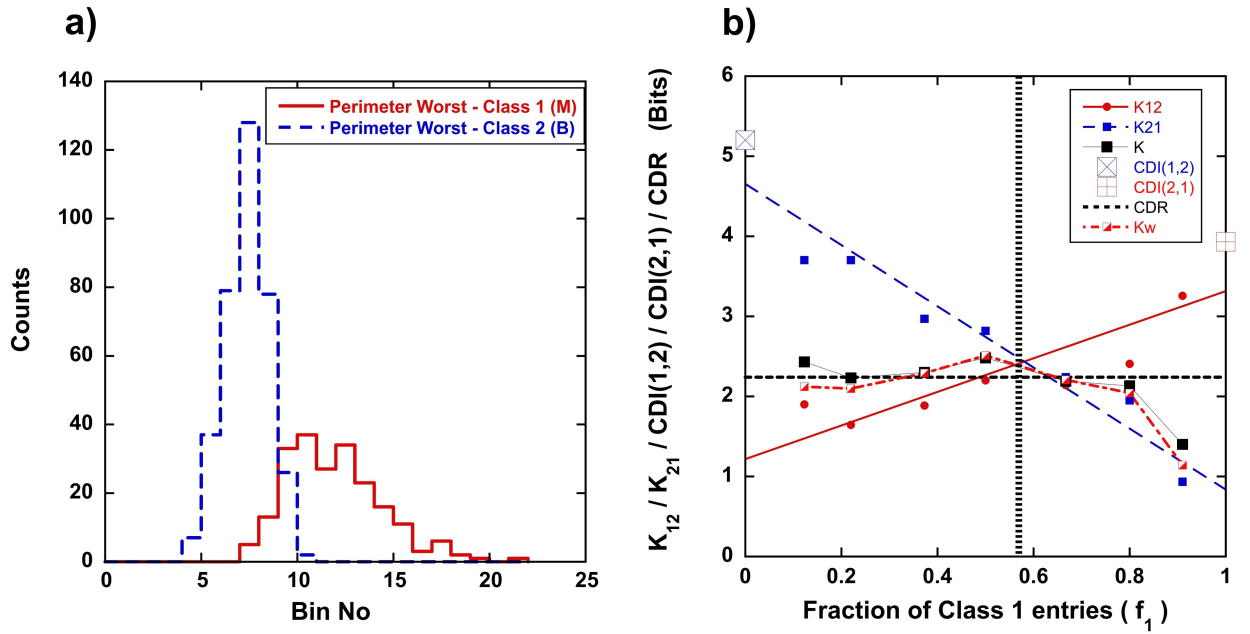


Figure 8: This figure shows an analysis of the “Perimeter Worst” variable for the Breast Cancer dataset. a) Histogram of the actual data for this variable with Class 1 (Malignant) in solid and Class 2 (Benign) in dashed lines. The bin width is 11.8 and binning starts at zero. The total number of entries is 569. b) This plot is similar to 7 a) but uses real data.  $f_B \simeq t_R = \frac{\text{CDI}(1,2)}{\text{CDI}(1,2) + \text{CDI}(2,1)}$  is 0.57 for this variable and is indicated by the vertical dashed line. It is not an accident that this is the point at which  $K_{12} \simeq K_{21}$ . See text for more detail.

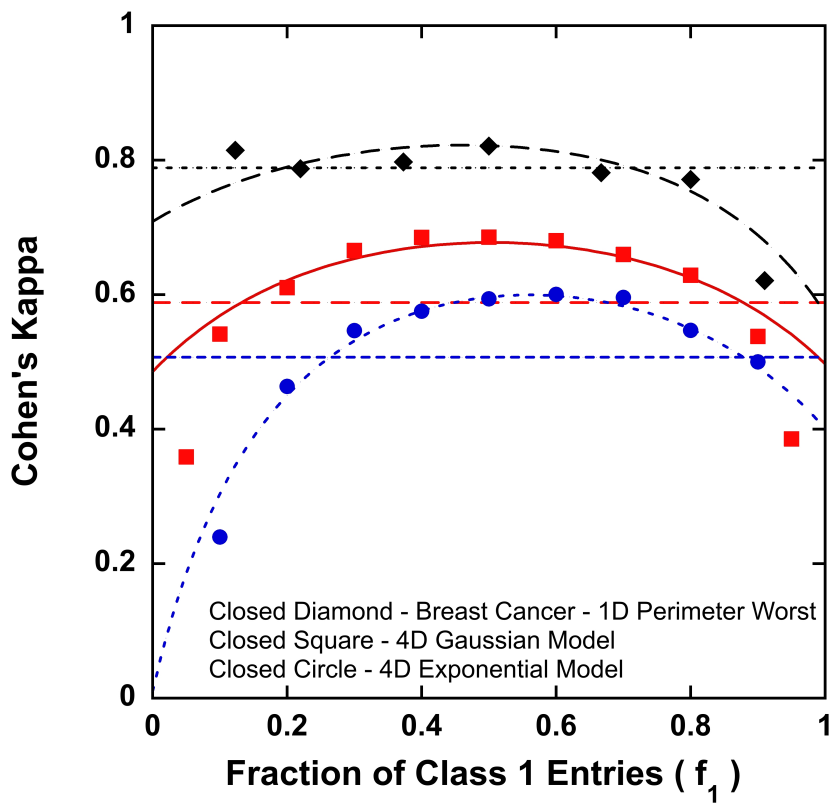


Figure 9: Cohen's Kappa as a function of the fraction of Class 1 entries for three datasets. The points are from the classification algorithm. The curves use the parameters extracted from Figs. 6a), 7a) and 8b), given in Table 3, and applying Equ. 3.22, Equ. 3.23 and Equ. 4.3.  $CDR$ , the kNN estimate of  $R(P, Q)$ , is shown by the dashed lines, and detailed in Table 4. See text for a full discussion.

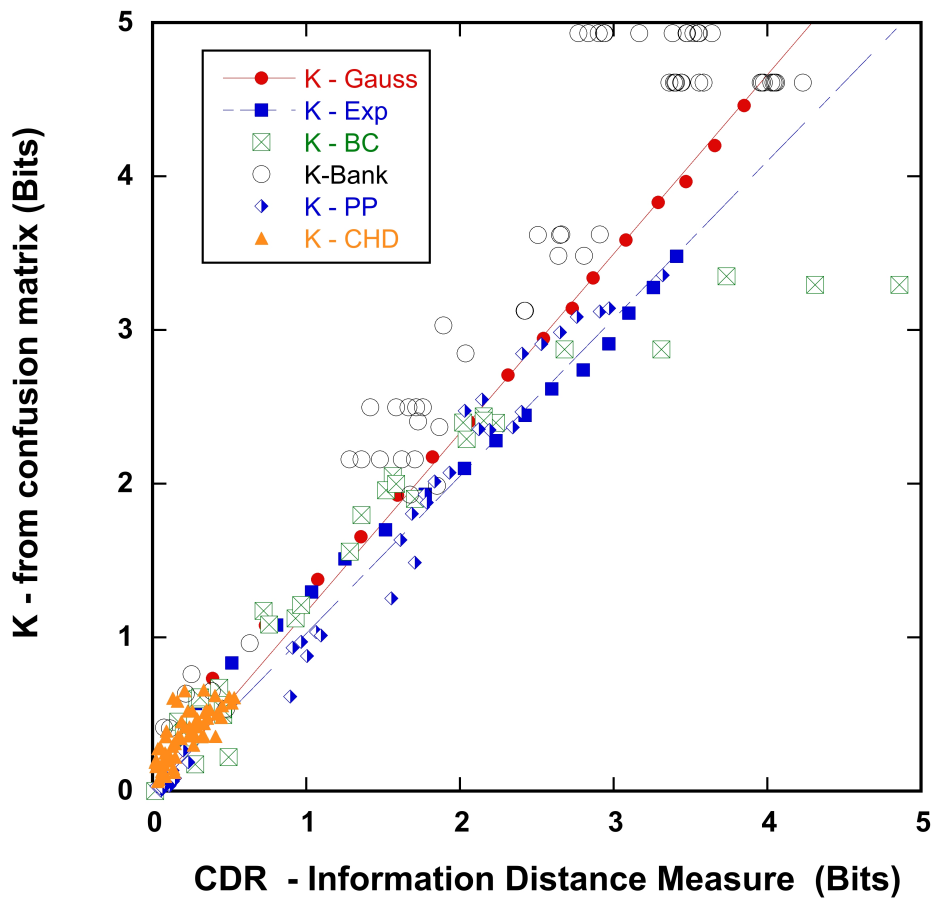


Figure 10: Average error rate,  $K$ , from the confusion matrix Cohen's Kappa, versus  $CDR$ , which is the kNN estimate of the Resistor Average Distance,  $R(P, Q)$ . This compares the classification algorithm performance versus the expected performance from an information theoretic distance. Gaussian (Closed Circle), Exponential (Closed square), Breast Cancer data (Crossed Open square), Bank data (Open circle), Particle Physics data (Half-filled diamond), Coronary Heart Disease data (Closed triangle). CHD data all below 0.5 bits. Line fits to the Gauss and Exponential data give slopes of 1.165 and 1.025.

## Kappa Scale

Very Good

Good

Moderate

Fair

Poor

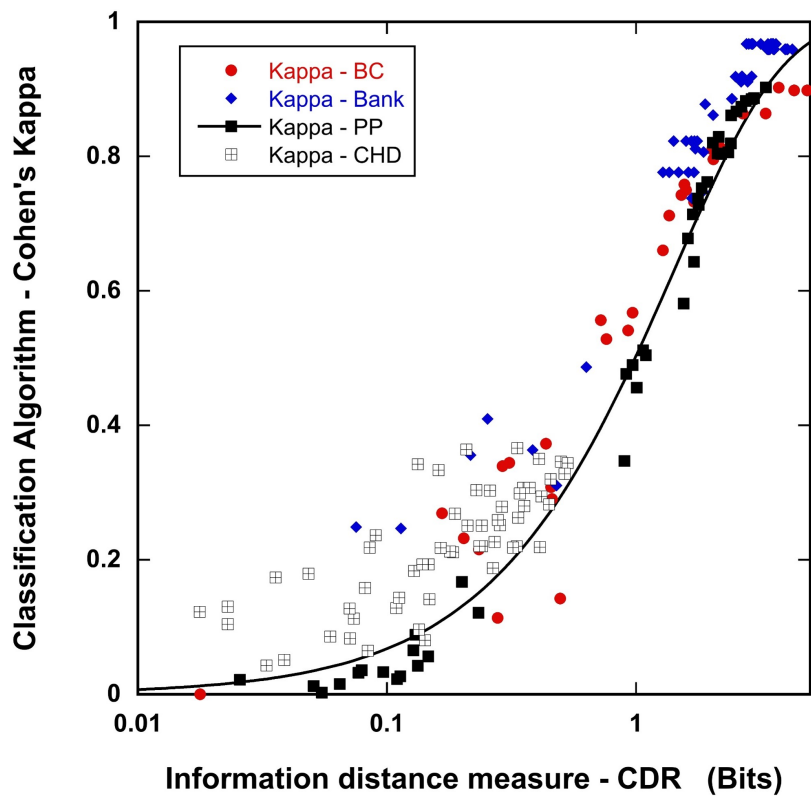


Figure 11: This figure combines the result of the classification algorithm performance using Cohen's Kappa versus the independently calculated,  $CDR$ , which is an estimate of the Resistor Average Distance,  $R(P, Q)$ , which is an information distance measure. The curve shows the relation,  $\kappa = 1 - 2^{-CDR}$ , Equ. 3.27. The points lie on this curve which indicates that the classification algorithm is performing as well as can be expected. The Kappa scale on the left hand side is from ref. [26]. The datasets are D1 to D4 detailed in Table 1.

# Tables

Table 1: Summary of Datasets

Data	Label	$N_1$ Class 1	$N_2$ Class 2	$N$	$f_1$	Continuous / Discrete	WEKA Algorithm [1]
16 Dim. Gauss	S1	8192	8192	16384	0.5	16/0	Bayes Network
16 Dim. Exp.	S2	8192	8192	16384	0.5	16/0	Bayes Network
Breast Cancer [19]	D1	212 (M)	357 (Be)	569	0.37	30/0	Simple Logistic Regression
Bankruptcy [20]	D2	107 (Bk)	143 (NBk)	250	0.43	0/6	J48 Decision Tree
Particle [17]	D3	3736 (B)	1264 (S)	5000	0.75	8/0	Random Forest
Heart Disease [21]	D4	302 (ND)	160 (CHD)	462	0.65	8/1	Logistic Regression

Table 2: Combination of variables used in each figure

Figure	Data	Combinations of variables	Combinations
4a	S1	V1,V1V2,V1V2V3,.....,V1V2....V15V16	16
4b	S2	V1,V1V2,V1V2V3,.....,V1V2....V15V16	16
5a	S1	As 4a	16
5a	S2	As 4b	16
6	S1	4D - V1V2V3V4	1
7	S2	4D - V1V2V3V4	1
8	D1	1D - Perimeter Worst	1
9	D1,S1,S2	In order - Perimeter Worst, 4D, 4D	3
10	S1	As 4a	16
10	S2	As 4b	16
10	D1	26 single variables + Selected; V1V2,V1V2V3,.....,V1V2...V7	32
10	D2	All combinations of 6 variables	63
10	D3	8 single, 25 pairs + Selected; V1V2V3,.....,V1V2V3....V8	42
10	D4	9 single, 36 pairs, 16 x 3 variable, 3 x 4 variable	64
11	D1, D2, D3, D4	As 10	201

Table 3: Confusion Matrix parameters - 4.3 and 4.5.1

DATA	$\hat{K}_{12}$ PARAMETERS		$\hat{K}_{21}$ PARAMETERS		Figs. 6a,7a, 8b
Units - Bits	$\Delta_1$	$D(2, 1)$	$\Delta_2$	$D(1, 2)$	
4D Gauss Model	$0.68 \pm 0.05$	$2.62 \pm 0.05$	$0.70 \pm 0.05$	$2.53 \pm 0.05$	
4D Exponential Model	$0.01 \pm 0.07$	$3.18 \pm 0.07$	$0.47 \pm 0.06$	$1.67 \pm 0.07$	
Breast Cancer - PW	$1.22 \pm 0.32$	$3.31 \pm 0.26$	$0.84 \pm 0.27$	$4.66 \pm 0.23$	

Table 4: kNN parameters - 4.3 and 4.5.1

Data	kNN PARAMETERS			Figs. 6a, 7a, 8b
Units - Bits	$CDI(1, 2)$	$CDI(2, 1)$	$CDR$	
4D Gauss Model	2.46	2.66	1.28	
4D Exponential Model	1.74	2.5	1.02	
Breast Cancer - PW	5.2	3.93	2.24	